University of Thi_Qar Journal for Engineering Sciences ISSN 2075-9746
http://www.doi.org/10.31663/tqujes.10.1.352(2019)
Vol10 No.1 (May 2019)

Available at http://jeng.utq.edu.iq
engjrnal@jeng.utq.edu.iq

Differential Quadrature Method for Dynamic behavior of Function Graded Materials pipe conveying fluid on visco-elastic foundation

Eman R. B[1], Talib. Eh. El[2], Sadiq. M.H[3]
[1] Department of Mechanical Engineer, College of Engineering, Thi-Qar University, Iraq
[2] Department of Mechanical Engineer, College of Engineering, Thi-Qar University, Iraq
[3] Department of Mechanical Engineer, College of Engineering, Thi-Qar University, Iraq

Abstract

The objective of this work is to study the dynamic behavior of FG pipe conveying fluid lying on the visco-elastic foundation using differential quadrature method. The material properties change constantly across the pipes thickness and depend on power law distribution. The vibration equations for FG pipe are obtained by using Hamilton's principle based on the Euler- Bernoulli model with (Clamped-Free) boundary conditions. An efficient numerical method by differential quadrature (GDQ) is developed to find the natural frequencies and stability for FG pipe. The effects gradient index and foundation parameters in fluid conveying FG pipes with certain flow velocity on frequencies are investigated. The present method of solution is accurately checked by comparing their results for fluid conveying pipe with the available results in the literature. From the comparison, a reasonable agreement was found. An increase in the gradient index results in an increase in the critical velocities for FG pipe.

Keywords: DQM, FGM pipe, visco-elastic foundation

1- Introduction

The dynamic behavior of piping convey fluid have been widely range of applied due to its extensive in different application such as industries, petroleum, chemical, aerospace, people's daily life, gasoline transportation systems, biological engineering systems, microfluidic, heat exchanger and Nano-fluidic devices [1]. The behavior of dynamic for pipes convey fluid had been studied by many researchers such as Chellapilla, K. R and Simha, H. S (2008) [2] investigated the vibrations behavior of fluid conveying pipes lying on the two-parameter foundation with different boundary conditions. They obtained that the Pasternak parameter of foundation tends to increase the fundamental frequency and the critical flow velocity also increase for the same Winkler constant. Tornabene F. et.al. (2010) [3] studied the stability of a cantilever fluid conveying pipe by using the (GDQ) method. They found that at a given value of the mass ratio, only one critical flow speed can exist for the system. Also, the results of this paper showed that this method can be conveniently used to perform parametric studies of the stability of various pipes conveying fluid. Lu, P, & Sheng, H (2012) [4] established exact Eigen equations for the problems of (clamped-clamped) and (simply supported) of pipe conveying fluid. The dynamic stability properties of the fluid structure coupled systems with and without considering the elastic foundation effect are discussed. A new analytical model for the dynamic behavior of a pipe conveying laminar flow with general boundary conditions was derived by Al-Hilli, A. H (2013) [5]. They found that the increase of the linear and rotational impedance leads to an increase in natural frequencies. Also when flow velocity equal zero or critical value, there is no difference in the frequency parameter for any value of the mass ratio. Mustafa, N. H (2014) [6] studied the dynamic stability for fluid-conveying pipe lying on the visco-elastic foundation with simply supported pipeline using the finite element method. The results showed that the increase in shear stiffness parameter leads to raising the value of the critical velocity of the fluid, while the increase in the damping parameter of foundation decreases it. A free vibration of the beam carrying fluid with axial motion and multiple supports was discussed by Kesimli A, et.al. (2016) [7]. Hamilton's principle was used to find the equations of motion and multiple time-scaled methods were used in the solution of vibration equation. According to these results, an increase in beam coefficient for all locations of support also increases the values of natural frequency. On the other hand, when the velocity of fluid increases, natural frequencies tend to decrease. Zare A, et.al (2017) [8] investigated the dynamic attitude of fluid-conveying pipes using Isogeometric analysis (IGA). The vibration equation was derived based on the Bernoulli- Euler theory and the virtual displacements were used in the analysis. Also, the rotary inertia terms were included in their derivation. The results showed that the Isogeometric approach gives the critical velocity of fluid high precision value for different conditions. Yun-dong, L, and Yi-ren, Y (2017) [9] studied the vibration analysis for fluid conveying pipe with elastic end conditions using the variation iteration method (VIM). They found the natural frequency, critical flow velocity and mode shape for different end conditions. Also, they demonstrated that VIM is efficient and high precision and the VIM can be also used for analysis of another gyroscope system. The dynamic behavior and stability for micro scale pipes conveying fluid with pinned-free boundary conditions were studied by Hu, K (2017) [10] using the differential quadrature (DQ) method. They were found the pinned-free flexible micro pipe was stable at low flow velocities. At high sufficiently flow velocities, the system becomes subject to flutter instability.

With the development of materials science and technology, a new type of composite materials, i.e. functionally gradient (FG) material, which has many excellent properties, has been made [11, 12], the mechanical behavior of FGM has been studied by researchers in past decades. Piovan, M. T and Sampaio, R (2008) [13] addressed the problem of vibrations for axial moving flexible beam made of FGMs and solved using the finite element method. The results showed that when the main beam component is ceramics there is high oscillatory deployment, but when the main beam component is metallic, the frequency of oscillation is lower. They show that this type of beam model is quite useful for the analysis of deploying beam, for both functionally graded and isotropic materials. Sina, S. A, et.al (2009) [14] developed the new theory of beam different from the traditional shear deformation theory for analyzed free vibration of function graded beam. They were found that the new beam theory is a little different in natural frequency from the first-order shear deformation theory. Alshorbagy, A, et.al (2011) [15] investigated the dynamic characteristics of the FGM beam using FEM. The virtual work principle with Bernoulli - Euler theory was used to drive the vibration equation. They found that the slenderness ratio has no effected on the vibration frequencies or mode shapes. Kim, Y. W (2005) [16] studied the effect of the temperature-dependent vibration characteristics of the FG rectangular plates. Rayleigh-Ritz procedure and 3rd SDT of plate were used to find the motion's equation. Numerical results confirmed that the characteristics of the vibration were significantly influenced by the plate geometry, composition of materials, and high temperature. The nonlinear free vibration of (FGM) Nano beams resting on the elastic foundation was studied by Vosoughi, A. R (2016) [17], DQM was applied to discretize the nonlinear vibration equation. The effect of the small scale parameter, boundary conditions, Length-to-height ratio and the foundation parameters on the nonlinear free vibration response of the FG Nano beams was investigated. Ebrahimi, F and Barati, M. R (2018) [18] investigated free vibration of FG Nano beams rested on viscoelastic foundation and subjected hydrothermal loading. They found that the viscoelastic foundation for (Clamped-Clamped) boundary condition has a larger critical damping coefficient as compared with (Clamped-pinned) and the later has larger critical damping coefficient than (pinned-pinned) FG Nano beam. Also, they obtained that the real and imaginary value of Eigen frequencies was reduced by increasing gradient index. Wang, Z. M and Liu, Y. Z (2016) [19] used the symplectic method to investigate the transverse vibration of FG pipe conveying fluid with clamped at both ends and Hamilton's principle was used to obtain the motion's equation. The effect of the gradient index on the critical flow velocity and complex frequency of FGM pipe conveying fluid was discussed. Deng, J. et.al (2017) [20] investigated the dynamic behaviors of a viscoelastic FG pipe conveying fluid with multi-span using the dynamic stiffness method. From the result, the influence of volume fraction exponent on the dynamic behaviors is clear when it is less than 10. Also, the results showed that the internal damping coefficient of the simply-supported FGM pipe had no effect on critical velocities. Tang, Y, and Yang, (2018) [21] studied the post-buckling and nonlinear vibration of a fluid-conveying FG pipe made. They found that the nonlinear frequency was increased with increased of the initial amplitude, but decreased as the flow velocity. In addition, both the critical flow velocity and the non-linear vibration frequency of the FGM pipe are rapidly decreasing with an increase in the gradient index of the material.

In this paper, the equation of motion is first examined for a pipe conveying fluid resting on viscoelastic and constructed with FGM using Euler- Bernoulli beam theory and Hamilton’s principle. Then, use a differential quadrature method; it is converted to solve eigen-problem (natural frequency). Also, performed the transverse dynamic characteristics and stability of a clamped–Free FG pipe conveying fluid for different flow velocity the power law

2- Mathematical formulation

Fig. 1 displays a schematic diagram for FGM pipe conveying fluid resting on a viscoelastic foundation. *L* is the length, h is thickness of pipe, (u) is the flow velocity, A_p and A_f respectively is the cross-sectional area of the FG pipe and the fluid, R_o and R_i is the outer and inner radius of the pipe. Symbols u and w represent the pipe displacement in the x and z directions, respectively. In derivation of this model, the pipe is assumed to obey Euler–Bernoulli Beam theory. The structure of the pipe has small deformation, the conveyed fluid is non-viscous and incompressible, the effects of gravity and internal damping are ignored and the power-law material property was considered as continuously varying across wall thickness direction of the pipe.

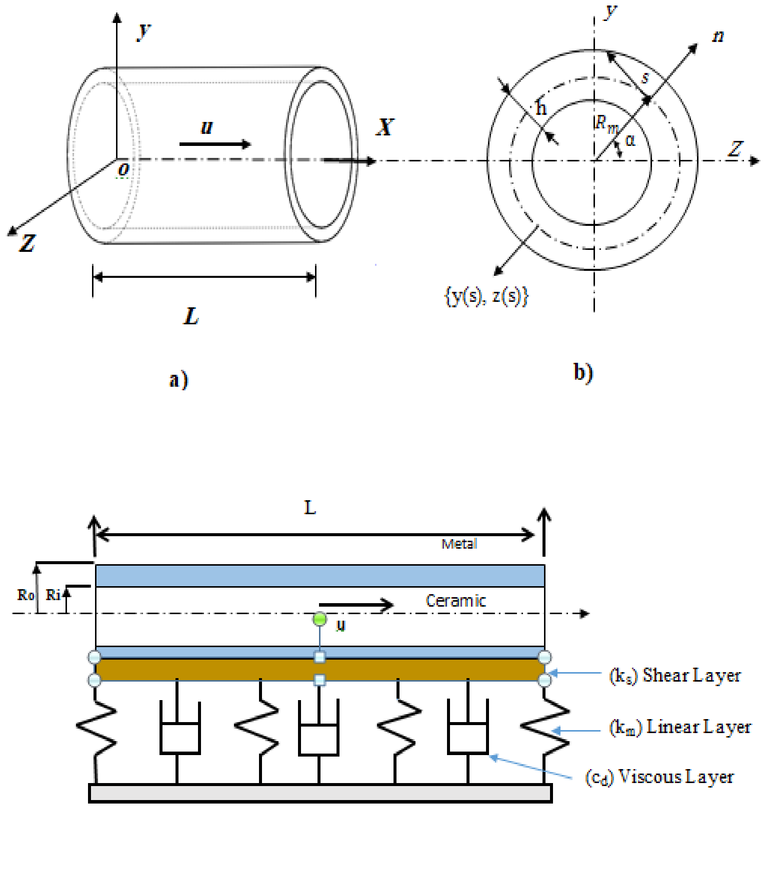

Fig. 1: (a) Side view of FGM pipe conveying fluid, (b) cross-section and coordinate system (n – s), and (c) Geometry of FGM pipe and visco-elastic foundation.

The dimensions and properties used in numerical results for FG pipe are taken as follows [21]. Aluminum and zirconium were selected respectively as metal materials (external) and ceramic (internal) of the FGM pipe. Their materials properties are given in Table-1. In this research Poisson's ratio (ν) is considered to be a constant and the value is $\nu = 0.3$

Table-1: Material properties of the constituents of FGM pipe

materials	ρ (kg/m^3)	E (GPa)	Radius (m)
Metallic (Outer)	2700	70	0.1
Ceramic (**I**nner)	3000	151	0.08

The effective function $F(n)$ of material properties are given by [22]:

$$F(n) = (F_o - F_i)\left(\frac{2n+h}{2h}\right)^k + F_i$$
$$V_i = \left(\frac{2n+h}{2h}\right)^k \quad \textbf{(1)}$$

Where (**n**) is a normal coordinate across the wall thickness (−h/2 ≤ n ≤h/2). The effective modulus of elasticity $E(n)$ and the effective density $\rho(n)$ for power law exponent are:

$$E(n) = (E_o - E_i)\left(\frac{2n+h}{2h}\right)^k + E_i \quad \textbf{(2)}$$

$$\rho(n) = (\rho_o - \rho_i)\left(\frac{2n+h}{2h}\right)^k + \rho_i \quad \textbf{(3)}$$

(**Fig.2)** shows the variation of volume fraction V_i along pipe thickness for different gradient index according to the relation in *Eqs* (1). It shows that when exponent (k = 0), a homogeneous pipe becomes; Also, the exponent k strongly affects the material properties of the FGM pipe.

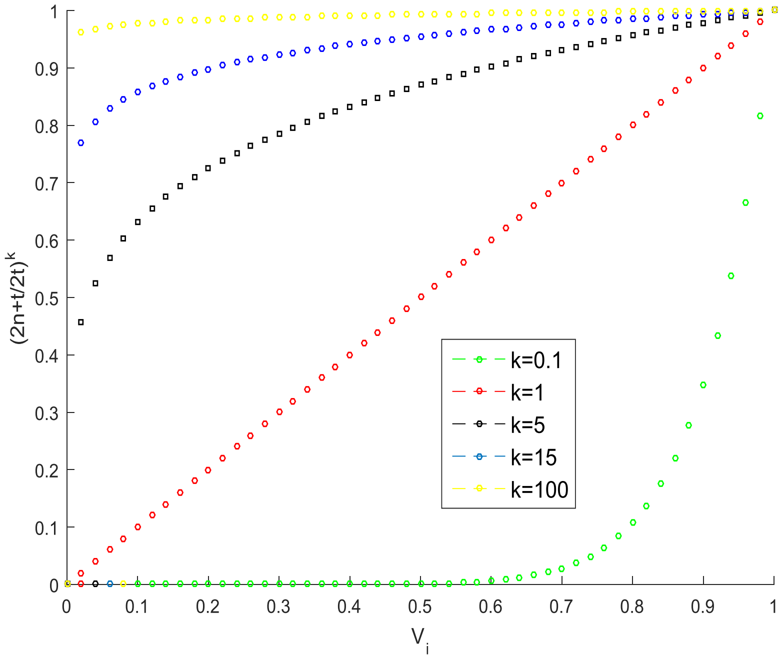

Fig. 2: Volume fraction variations along the thickness of pipe for different values of power gradient index (k).

To derive the equation of motion, the energy principle and the variation approach will be used. To this end, the kinetic energy for internal fluid flow T_f is written as follows [23]:

$$T_f = \frac{1}{2}\int_0^L m_f \left[\left(\frac{\partial w}{\partial t} + V_f \frac{\partial w}{\partial x}\right)^2 + V_f^2\right] dx \quad \textbf{(4)}$$

Where m_f is represented the mass density for fluid

$$m_f = \rho_f A_f \quad \textbf{(5)}$$

The kinetic energy's for the FG pipe can be expressions as [23]:

$$T_p = \frac{1}{2}\int_0^l m_p \left(\frac{\partial w}{\partial t}\right)^2 dx \quad \textbf{(6)}$$

where m_p is represented the effective mass of pipe, the effective of pipe mass can be written as

$$\begin{aligned} m_p &= \int_0^{2\pi R_m}\int_{-h/2}^{h/2} \rho(n)\frac{R_m + n}{R_m} dsdn \\ &= \int_0^{2\pi R_m}\int_{-h/2}^{h/2} \left[(\rho_o - \rho_i)\left(\frac{2n+h}{2h}\right)^k + \rho_i\right]\left(1 + \frac{n}{R_m}\right) dnds \\ &= m^* \rho_k \end{aligned} \quad \textbf{(7)}$$

Where

$$m^* = 2\pi R_m h \rho_m, \rho_k = \frac{1 + \rho_R k}{k+1} + h_R(1 - \rho_R)\left(\frac{1}{k+1} - \frac{1}{2(k+1)}\right) \quad \textbf{(8)}$$

$$\rho_R = \frac{\rho_c}{\rho_m}, h_R = \frac{h}{R_m}, E_R = \frac{E_c}{E_m}$$

The total kinetic energy is defined as $T = T_p + T_f$ and its variation δT is obtained as:

$$T = \int_0^L \frac{1}{2} m_p \left(\frac{\partial w}{\partial t}\right)^2 dx + \int_0^L \frac{1}{2} m_f \left[\left(\frac{\partial w}{\partial t} + V_f \frac{\partial w}{\partial x}\right)^2 + V_f^2\right] dx \tag{9}$$

$$\delta T = m_p \int_0^L \frac{\partial w}{\partial t}\frac{\partial \delta w}{\partial t} dx + m_f \int_0^L \left(\frac{\partial w}{\partial t}\frac{\partial \delta w}{\partial t} + V_f \frac{\partial w}{\partial t}\frac{\partial \delta w}{\partial x} + V_f \frac{\partial w}{\partial x}\frac{\partial \delta w}{\partial x}\right) dx \tag{10}$$

Assuming that the pipeline is elastic, the stress – strain relation is given by:

$$\sigma_x = \frac{E(n)}{1-v^2}\varepsilon_x \tag{11}$$

The transverse displacements along $u_{(x,t)}$ is written as follows:

$$u_{(x,t)} = -y\frac{\partial w}{\partial x} = -\left(Y(s) - n\frac{dZ}{ds}\right)\frac{\partial w}{\partial x} \tag{12}$$

According to small deformation assumption, the axial strain is written as:

$$\varepsilon_x = \frac{\partial u_x}{\partial x} = -\left(Y(s) - n\frac{dZ}{ds}\right)\frac{\partial^2 w}{\partial x^2} \tag{13}$$

Then, the expression of strain energy for FG pipe is obtained as:

$$U_s = \frac{1}{2}\int_0^L \int_{-h/2}^{h/2} \int_0^{2\pi} \sigma_x \varepsilon_x (R_m + n) d\theta dn dx \tag{14}$$

$$U_s = \frac{1}{2}\int_0^L \int_{-h/2}^{h/2} \int_0^{2\pi Rm} \sigma_x \varepsilon_x \left(\frac{R_m + n}{R_m}\right) ds dn dx \tag{15}$$

Now, substituting *Eqs* (11) and (13) in *Eqs* (15), and perform some manipulation, the bending strain energy is expressed in terms of pipe deflection as follows:

$$U_s = \frac{1}{2}\int_0^l \alpha \left(\frac{\partial^2 w}{\partial x^2}\right)^2 dx \tag{16}$$

where α is the flexural stiffness for FGM pipes, i.e.

$$\alpha = \pi R_m^3 A_1 + 2\pi R_m^2 A_2 + \pi R_m A_3$$

$$A_1 = \frac{1}{1-v^2}\int_{-\frac{h}{2}}^{\frac{h}{2}} E(n)\left(1 + \frac{n}{R_m}\right) dn,$$

$$A_2 = \frac{1}{1-v^2}\int_{-\frac{h}{2}}^{\frac{h}{2}} E(n)\left(1 + \frac{n}{R_m}\right) n dn \tag{17}$$

$$A_3 = \frac{1}{1-v^2}\int_{-\frac{h}{2}}^{\frac{h}{2}} E(n)\left(1 + \frac{n}{R_m}\right) n^2 dn$$

the flexure stiffness of FG pipe is written as:

$$\alpha = \alpha' J_k \tag{18}$$

$$J_k = \frac{1}{1+0.25h_R^2}\left[\begin{array}{l} \frac{1+E_R k}{k+1} + 3(1-E_R)h_R\left(\frac{1}{k+2} + \frac{1}{2(k+1)}\right) \\ + 3(1-E_R)h_R\left(\begin{array}{l}\frac{1}{k+3} + \frac{1}{k+2} \\ + \frac{1}{4(k+1)}\end{array}\right) \\ + \frac{1}{4}E_R h_R + \\ 3(1-E_R)h_R^2\left(\begin{array}{l}\frac{1}{k+4} + \frac{1}{2(k+3)} + \\ \frac{1}{4(k+2)} + \frac{1}{8(k+1)}\end{array}\right)\end{array}\right] \tag{19}$$

$$\alpha' = \frac{(1+0.25h_R^2)\pi E_m R_m^3 h}{1-v^2}$$

The variation of δU_s is written as:

$$\delta U_s = \alpha \int_0^L \frac{\partial^2 w}{\partial x^2}\frac{\partial^2 \delta w}{\partial x^2} dx \tag{20}$$

The virtual work δW^{ext} done by the external transverse forces F^{ext} exerted on the FG pipe by the viscoelastic foundation can be calculated as:

$$\delta W^{ext} = \int_0^L F^{ext}\,\delta w\,dx$$

$$F^{ext} = k_s \frac{\partial^2 w}{\partial x^2} - c\frac{\partial w}{\partial t} - k_m w \qquad (21)$$

$$\delta W^{ext} = \int_0^L \left(k_s \frac{\partial^2 w}{\partial x^2} - c\frac{\partial w}{\partial t} - k_m w\right)\delta w dx$$

2-1 Hamilton principle

The general form of Hamilton's principle for pipes conveying flow was given by Benjamin [24], the dynamic version of a virtual displacements principles or Hamilton's principle is:

$$\delta\int_{t_1}^{t_2}(T - U_s + W^{ext})\,dt \qquad (22)$$

$\delta w = 0$ at $t = t_1 = t_2$

Substituting *Eqs* (10), (20) and (21) into *Eq*s (22), integrating by parts and presenting the coefficients of δw zero, lead to the vibration equations as:

$$\alpha\frac{\partial^4 w}{\partial x^4} + \left[m_f V_f^2 - K_S\right]\frac{\partial^2 w}{\partial x^2} + 2V_f m_f\frac{\partial^2 w}{\partial x\partial t} + \left[J_\rho + m_f\right]\frac{\partial^2 w}{\partial t^2} + C_d\frac{\partial w}{\partial t} + K_M w = 0 \qquad (23)$$

Clamped–free (C–F) is used to show the effects of end stiffness on the vibrational characteristics of FG pipe conveying fluid lying on viscoelastic foundation.

Clamped-Free:

$$w(0,t) = \frac{\partial w(0,t)}{\partial x} = 0, \qquad \frac{\partial^2 w(L,t)}{\partial x^2} = \frac{\partial^3 w(L,t)}{\partial x^3} = 0 \qquad (24)$$

For convenience, these equations can be written dimensionless by using the following definition:

$$\eta \to \frac{x}{L},\ W \to \frac{w}{L},\ \tau \to \frac{t}{L^2}\left(\frac{\alpha'}{m_f + m^*}\right)$$

$$u \to V_f L\sqrt{\frac{m_f}{\alpha'}},\ \beta \to \frac{m_f}{m_f + m^*}$$

$$K_M \to \frac{L^4}{\alpha'}K_m,\ k_s \to \frac{L^2}{\alpha'}K_S \qquad (25)$$

$$C \to \frac{C_d L^2}{\sqrt{\alpha'(m_f + \alpha')}}$$

Substituting the dimensionless parameters *Eq*s (25) into *Eq*s (23), the linear dimensionless form of the vibration equation is acquired:

$$J_k\frac{\partial^4 W}{\partial\eta^4} + \left[u^2 - K_S\right]\frac{\partial^2 W}{\partial\eta^2} + 2u\beta^{\frac{1}{2}}\frac{\partial^2 W}{\partial\eta\partial\tau} + \left[\beta + (1-\beta)\rho_k\right]\frac{\partial^2 W}{\partial\tau^2} + C_d\frac{\partial W}{\partial\tau} + K_M W = 0 \qquad (26)$$

The C–F dimensionless forms are readily studied as:

$$W(0,\tau) = \frac{dW(0,\tau)}{d\eta} = 0, \qquad \frac{d^2W(1,\tau)}{d\eta^2} = \frac{d^3W(1,\tau)}{d\eta^3} = 0 \qquad (27)$$

2-2 Differential quadrature method

The DQM is a numerical method, and it requires less grid points and then less computer time and storage to obtain acceptable accuracy. Successful applications of the DQM in many engineering problems have been demonstrated by numerous researches [25, 26]. The key procedure in the application of DQ lies in a determination of the weighting coefficients [25], so that its first derivative $f_x^{(1)}(x)$ at any grid point over [a, b] can be found by the following approximation:

$$f_x^{(1)}(\eta) \cong \sum_{j=1}^{N} C_{ij}^{(1)} f(x_j),,,, i = 1,2,.... N \qquad (28)$$

where the coefficient matrix $C_{ij}^{(1)}$ can be specified in various fashions $f_\eta^{(1)}(x)$ finds the first order derivative of $f(x)$ with respect to x at x_i presented by Bellman et al (1972) [27]. For generality, GDQ chooses the base polynomials (or test functions) $g_k(\eta)$ to be the Lagrange interpolating polynomial:

$$g_k(\eta) = \frac{M(\eta)}{(\eta - \eta_k) M^{(1)}(\eta_k)} \tag{29}$$

Where

$$M(\eta) = \prod_{i=1}^{N} (\eta - \eta_j),, M^{(1)}(\eta) = \prod_{i=1, i\neq k}^{N} (\eta_k - \eta_j) \tag{30}$$

With these assumptions, *Eq*s (29) converts to:

$$g_k(\eta) = \frac{N(\eta, \eta_k)}{M^{(1)}(\eta_k)} \tag{31}$$

The First order derivatives of the smooth function may be written as:

$$C_{ij}^{(1)} = \frac{N^{(1)}(\eta_i, \eta_j)}{M^{(1)}(\eta_j)} \tag{32}$$

Substituting this expression in Eq. (32), we get

$$C_{ij}^{(1)} = \begin{cases} \dfrac{M^{(1)}(\eta_i)}{\eta_i - \eta_j}; i \neq j \\ \dfrac{M^{(2)}(\eta_i)}{2M^{(1)}(\eta_i)} i = j \end{cases} \tag{33}$$

The computation of $C_{ij}^{(1)}$ without the restriction of choosing grid points η_i can be found from the expression of *Eq*s (33). Rather than evaluating $M^{(2)}(\eta_i)$, it is worth to mention that one set of base polynomials can be derived uniquely by linear combination of another set of base polynomials in a vector space.

The second and higher order derivatives of the smooth function may be written with the linear constrained relationships as [28].

$$f_\eta^{(m)}(\eta_i) \cong \sum_{i=1}^{N} C_{ij}^{(m)} f(\eta_j),,, i = 1,2,..., N \tag{34}$$

Then, the (m^{th}) order derivatives can be expressed as

$$f_\eta^{(m-1)}(\eta_i) \cong \sum_{i=1}^{N} C_{ij}^{(m-1)} f(\eta_j),,, i = 1,2,..., N \tag{35}$$

Now let us substitute *Eqs* (29) in *Eqs* (34) and (35) and using *Eqs* (33), and (31), the recurrence relation is written as follows

$$C_{ij}^{(m)} = \begin{cases} m\left(C_{ij}^{(1)} C_{ii}^{(m)-1} - \dfrac{C_{ij}^{(m)-1}}{\eta_i - \eta_j} \right); i \neq j \\ \dfrac{M^{(m+1)}(\eta_i)}{(m+1) M^{(1)}(\eta_i)}; i = j \end{cases} \tag{36}$$

In N-dimensional vector space, the system of equations for $C_{ij}^{(m)}$ derived from Lagrange interpolating polynomials.

2-3 Discretization of governing equation

The non-homogeneous grid points in case of DQM are to be considered as Chebyshev-Gauss-Lobatto [29] points in axial direction. The governing equation (*Eq*s (26)) for free vibration of FG pipes conveying fluid lying on the viscoelastic foundation can be transformed into the following expression by substituting the weighting coefficients of required derivatives

$$\begin{aligned} &J_k \sum_{j=1}^{N} C_{ij}^{(4)} W_j + (u^2 - k_S) \sum_{j=1}^{N} C_{ij}^{(2)} W_j \\ &+ 2\lambda u \sqrt{\beta} \sum_{j=1}^{N} C_{ij}^{(1)} W_j \\ &+ \left(c\lambda + [\beta + (1-\beta)\rho_k]\lambda^2 + k_m\right) W_j = 0 \end{aligned} \tag{37}$$

where $j = 1,2,..., N$; the boundary conditions at x =0 and L stated in *Eqs* (27) becomes:

Clamped-Free:

$$\begin{aligned} &\eta = 0, W_1 = \sum_{j=1}^{N} C_{1j}^{(1)} W_j, \\ &\eta = 1, \sum_{j=1}^{N} C_{Nm}^{(2)} W_m = -\sum_{j=1}^{N} C_{Nj}^{(3)} W_j \end{aligned} \tag{38}$$

By utilizing the DQM, *Eqs* (43) and (48) can be transformed to an assembled form given as follows:

$$\begin{aligned} &\begin{bmatrix} [K_{bb}] & [K_{bd}] \\ [K_{db}] & [K_{dd}] \end{bmatrix} \begin{Bmatrix} \{w_b\} \\ \{w_d\} \end{Bmatrix} + \begin{bmatrix} [0] & [0] \\ [C_{db}] & [C_{dd}] \end{bmatrix} \begin{Bmatrix} \{\dot{w}_b\} \\ \{\dot{w}_d\} \end{Bmatrix} \\ &+ \begin{bmatrix} [0] & [0] \\ [M_{db}] & [M_{dd}] \end{bmatrix} \begin{Bmatrix} \{\ddot{w}_b\} \\ \{\ddot{w}_d\} \end{Bmatrix} = \{0\} \end{aligned} \tag{39}$$

In which the subscript *b* represents the displacements associated with the boundary points (at the two ends of the CNT conveying fluid), while *d* represents the remainder. The dot denotes the time derivative. For a self-excited vibration, the solution of *Eqs* (45) can be written as

$$\{w\} = \{\overline{w}\}\exp(\lambda t) \tag{40}$$

Where λ is the complex eigenvalue and written:

$$\lambda = \mathrm{Re}(\lambda) + \mathrm{Im}(\lambda)$$
$$\{\overline{w}\} = \{\{\overline{w}_b\}, \quad \{\overline{w}_d\}\}^T \tag{41}$$

and $\{\overline{w}\}$ is defined as an undetermined function of vibration amplitude. For solving Eq (39), the results presented that the eigenvalues are generally complex quantities, It should be noted that the $\lambda = \mathrm{Im}(\lambda)$ is the system frequency of FG pipe while $\lambda = \mathrm{Re}(\lambda)$ relates to system decaying rate and demonstrations its stability. The positive values of the real part express the instability region and the negative values means that the system is in stable condition. Substitution of *Eq*s (40) into *Eq*s (39) yields a homogeneous equation, which corresponds to the following eigenvalue problem

$$\left(\lambda^2[M] + \lambda[C] + [K]\right)\{\overline{w}_d\} = \{0\} \tag{42}$$

By reducing the order of *Eq*s (42), the quadratic eigenvalue problem given in *Eq*s (42) can be reformulated as a linear eigenvalue problem as follows:

$$[A]\{\overline{X}\} = \lambda[B]\{\overline{X}\} \tag{43}$$

Where

$$[A] = \begin{bmatrix} -[K] & [0] \\ [0] & [M] \end{bmatrix}, \quad [B] = \begin{bmatrix} [C] & [M] \\ [M] & [0] \end{bmatrix} \text{ and } \quad \{\overline{X}\} = \begin{Bmatrix} \overline{w}_d \\ \lambda\overline{w}_d \end{Bmatrix} \tag{44}$$

The function "eigs" in MATLAB was adopted to obtain the eigenvalues and eigenvectors for *Eq*s (23). In general, the eigenvalues of the present system is complex, its real part indicates an attenuation or amplification factor of the vibration amplitude due to the dissipation or supply of the energy from the flow, and the imaginary part represents the natural frequency of the system.

3-Results of vibration for FG pipe

Based on the DQM, the linear frequency and critical fluid velocity of the embedded FG pipe are obtained in this study. Firstly, the validity of the present analysis was checked by comparing the results for homogenous pipe on two parameter foundations with those obtained by Chellapilla, K. R and Simha, H. S [2]. A comparison between present and previous values of natural frequencies in the first four modes is given in **Table 2**, and **Table 3** depicts the first fourth eigenvalue of FG pipe conveying fluid flow with varying total numbers of grid points in the DQM for the C-F boundary conditions. It is seen that the results are convergence when (*N* =17) and they improved by increasing the number of grid points. It is noted that (*N*=20) is used in all Figures and Tables appear in this thesis. From **Tables 2** and **3**, it can see that the results converge rapidly by increasing the sampling points and also, close agreement exists between the present solution and the results of exact solution and Fourier series [20].

Table-2: Comparison between the first dimensionless natural frequencies of a homogenous pipe with (P-P) and (C-C) end condition $(u = k = k_s = c_d = 0)$.

BC		Pinned-pinned					
		k_m					
β	u	0.5		2.5		10	
		Present work	Ref[2]	Present work	Ref [2]	Present work	Ref [2]
0.1	0	9.894	9.895	9.995	9.995	10.363	10.364
	1	9.3735	9.374	9.479	9.48	9.866	9.866
	2	7.6115	7.612	7.740	7.741	8.206	8.207
0.3	0	9.894	9.895	9.995	9.995	10.363	10.364
	1	9.354	9.355	9.460	9.461	9.846	9.847
	2	7.547	7.549	7.675	7.677	8.138	8.139
0.5	0	9.894	9.895	9.995	9.995	10.363	10.364
	1	9.336	9.337	9.441	9.442	9.827	9.828
	2	7.485	7.487	7.612	7.614	8.071	8.073
BC	Clamped-clamped						
		k_m					
β	u	0.5		2.5		10	
		Present work	Ref[2]	Present work	Ref[2]	Present work	Ref[2]
0.1	0	22.384	22.384	22.431	22.429	22.598	22.596
	1	22.093	22.093	22.14	22.138	22.308	22.307
	2	21.195	21.197	21.242	21.244	21.417	21.419
0.3	0	22.383	22.384	22.431	22.429	22.598	22.596
	1	22.062	22.063	22.109	22.108	22.277	22.276
	2	21.076	21.08	21.122	21.126	21.296	21.3
0.5	0	22.382	22.384	22.431	22.429	22.598	22.596
	1	22.032	22.033	22.079	22.078	22.247	22.246
	2	20.958	20.960	21.005	21.008	21.178	21.180

Table-3: Natural frequency of pipes for cantilever boundary condition at u = 0.

N	λ_1	λ_2	λ_3	λ_4
5	4.75071	-	-	-
7	3.48659	21.42848	66.99381	-
9	3.51674	22.19796	56.69972	107.31805
11	3.51621	22.03653	62.56575	139.72182

17	3.51621	22.03773	61.70093	120.90238
20	3.5160	22.0346	61.6974	120.9020
Exact [20]	3.5160	22.0345	61.6972	120.9019

3-1 Effect of the flow velocity

This subsection investigates the natural frequency of clamped-free end condition of FG pipe by varying the fluid velocity. **Table 4** presents the dimensionless vibration frequency as a function of the dimensionless flow velocity. The results are computed for the case of $k = 1$ and $k_m = 0.01, k_s = 0.01, c_d = 0.01$. As shown in this table, with increasing of u the results of the first three vibrations frequency decreased (i.e. the natural frequencies of FG pipe conveying flow is dependent on the fluid velocity (u).

Table 4: Effect of flow velocity (u) on the lowest three natural frequencies.

B.C	u	λ_1	λ_2	λ_3
Clamped-Free	0	4.9044	30.7358	86.0612
	1	4.8228	30.5439	85.8211
	2	4.5729	29.9660	85.0986
	3	4.1376	28.9954	83.8876

Table 5 shows the critical velocities of FGM pipe with $(K_m = 50, K_s = 10, C_d = 10)$ for C-F boundary conditions and **Fig. 3** depicts the lowest three modes as functions of fluid velocity u with C-F end condition. It can be found from **Table 5** that the critical velocity is increased with the increased of exponent k. It also can be observed from (**Fig. 3**), that the natural frequencies increased with increment exponent k. It could be concluded that the stability of FGM pipe increase with increasing exponent k. This is due to the verity that the content of Zirconia in FGM pipe increases whiles the content of Al decreases with increasing exponent k, and the Young's modulus of Zirconia is much larger than that of Al. The FGM pipe displays some more complex and interesting dynamical behaviors when the exponent k=10. The divergence of first mode occurred at u=4.05 for cantilever pipe. On the other hand, it is also found that the exponent k can easily alter distributions of natural frequencies of FGM pipe conveying fluid.

(a)

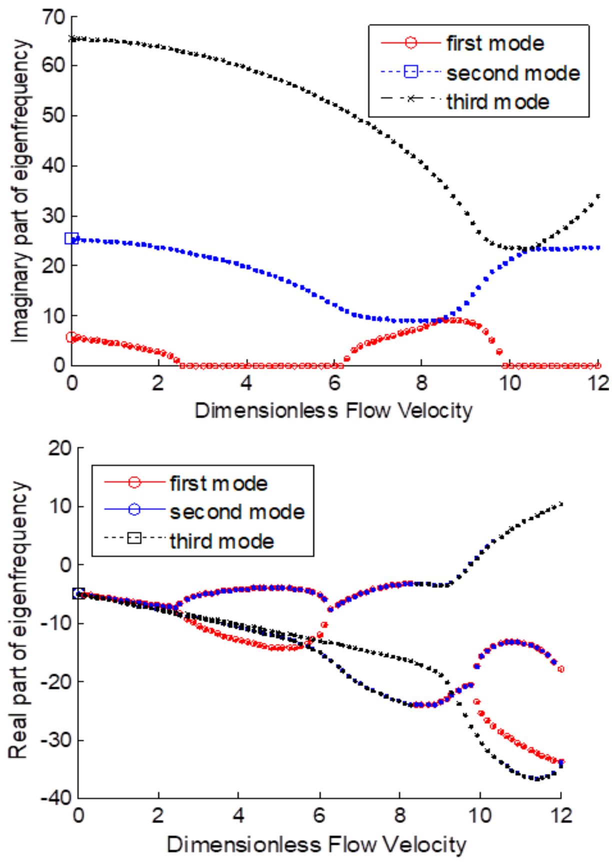

(b)

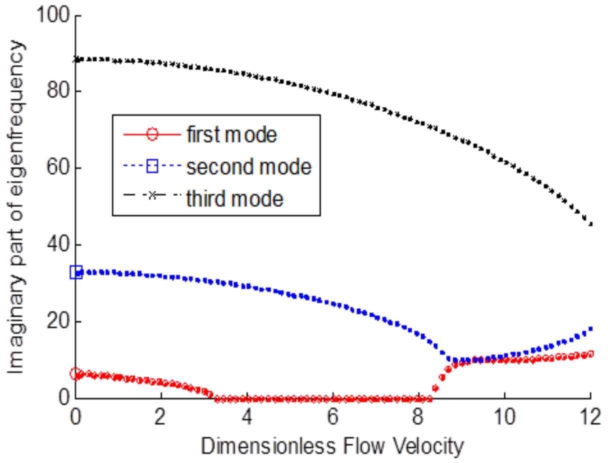

Table 5: Critical velocities for FG pipe for different exponents' k $(K_m = 50, K_s = 10, C_d = 10)$.

Critical velocity	B.C	k=0	k=1	k=10
u_{d1}	C-F	2.25	3.15	4.05

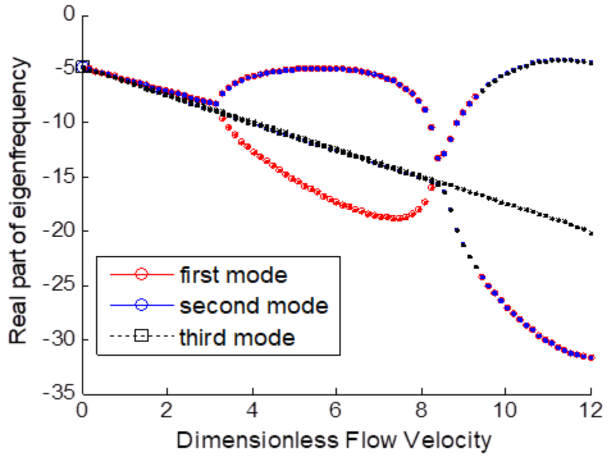

(c)

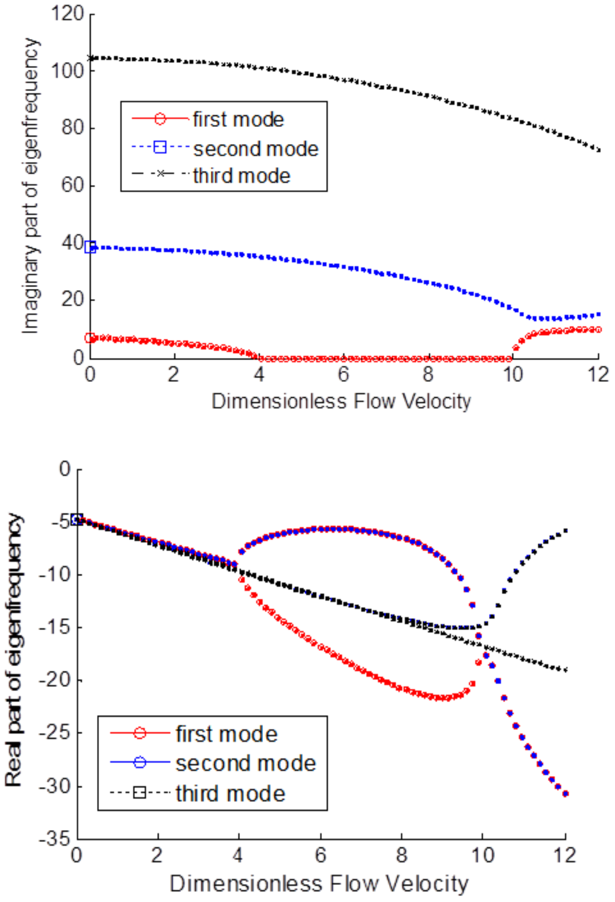

Fig. 3: Lowest three modes of cantilever FGM pipe lying on visco-elastic foundation against fluid velocity (*u*) $(K_m = 50, K_s = 10, C_d = 10)$ (a) exponent *k*=0, (b) exponent *k*=1, (c exponent *k*=10.

The components of the natural frequency for a cantilevered FG pipe convey fluid with dimensionless fluid velocity at the various value of volume fraction exponent (k=0, 3, and 10) are presented in (**Fig. 4**), for numerical calculations in this case $(K_m = 50, K_s = 10, C_d = 10)$ We note that, the imaginary part of vibration frequency and the critical of flow velocity will increase with an increase in volume fraction index k. Also, from this figure, it is noted that the dimensionless frequency decreases with an increase in fluid velocity. This is because higher fluid velocities weaken the structure's stiffness.

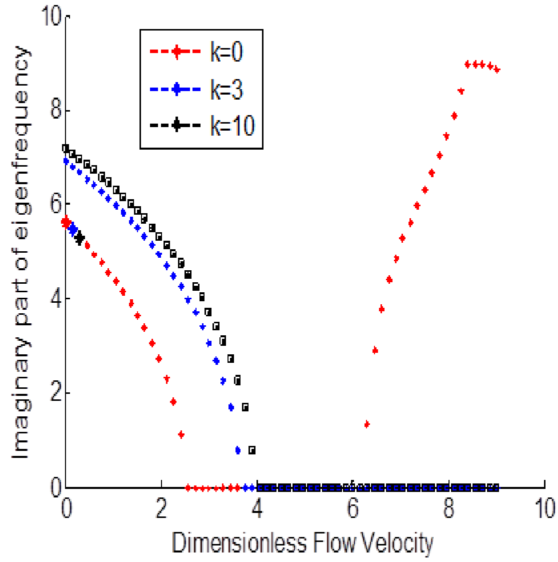

Fig. 4: The first mode of (C-F) FG pipe lying on visco-elastic foundation against fluid velocity *u* for different values of gradient index k $(K_m = 50, K_s = 10, C_d = 10)$.

3-2 Effect of the power law exponent

This subsection demonstrated the effect of gradient index k on natural frequency of clamped-free end conditions of FG pipe with varies flow velocity. The continuously graded variation of physical properties of FGM in the composition of ceramic and aluminum phases across the wall thickness with a simple power law is considered. When the power law exponent k = 0 the pipe is made of the metal material and when k⟶ + ∞, the pipe is made of the ceramic material, respectively. Table-6 and Fig. 5 shows the effect of gradient index (k) and dimensionless flow velocity (u) on the first natural frequency of FGM pipe for (C-F) condition with $(K_m = 50, K_s = 10, C_d = 10)$. This result shows that the increase for the gradient index leads to a decrease in natural frequency values of imaginary part. While vibration frequency of FGM pipe is increased with the increased in the exponent of volume fraction k. This is generally due to the fact that zirconia content in FGM pipe increases, whilst the aluminum content decrease with an increasing the exponent, and the zirconia Young's modulus is frequently greater than that from aluminum.

Table-6: The effect of volume fraction index (k) and flow velocity on first eigenvalue for C-F boundary condition.

B.C	u	k				
		0	2	5	10	100
C-F	0	3.51621	5.29359	5.66661	5.83415	6.01427
	2	2.98870	4.99520	5.39794	5.57758	5.76993
	4	0.78813	4.037720	4.548082	4.770337	5.00509

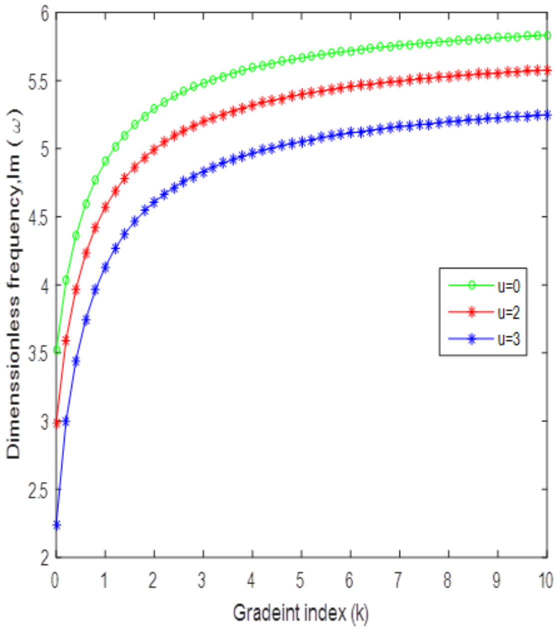

Fig. 5: Effect of power law exponent (k) on imaginary natural Frequency with different flow velocity (u) ($K_m = 50$, $K_s = 10$, $C_d = 10$) for (C-F) boundary condition.

(a)

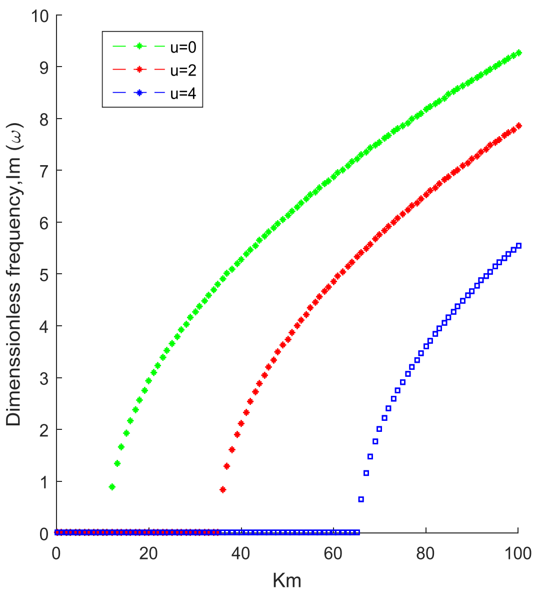

(b)

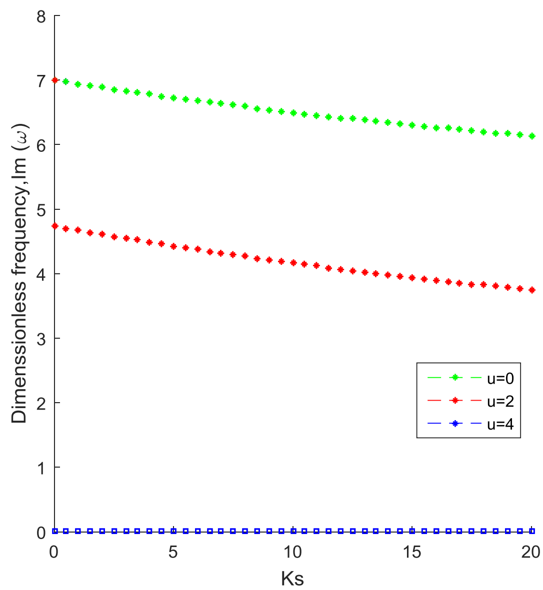

3-3 Effect of Viscoelastic Foundation parameter

This subsection demonstrated the effect of viscoelastic foundation parameter on natural frequency of (clamped-free) FG pipe with different dimensionless flow velocity. **Fig. 6** shows the effect of coefficients (K_m, K_s, C_d) in the standard viscoelastic model on the imaginary part of frequency with different flow velocity. The results indicated that increasing K_m and K_s leads to improved stiffness of system and consequently the stability increases while the imaginary part of frequency decreases with an increase of foundation viscous damping C_d.This is because the increment of foundation viscous damping leads to the reduction of dynamic properties of the pipe structure. As can be seen, the influence of K_m on system stiffness is higher than K_s. This is due to the fact that increasing elastic coefficient increases the system stiffness.

(c)

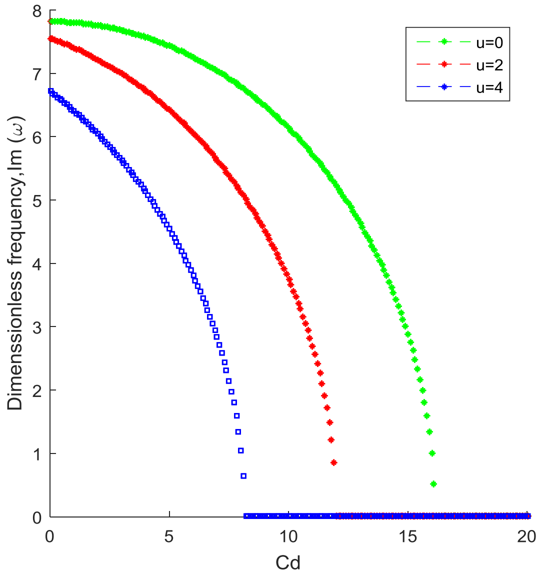

Fig. 6: Effect of visco-elastic foundation parameter on first natural frequency for (C-F) FG pipe with different flow velocity u, a) $(K_s = 20, C_d = 10, k = 1)$, b) $(K_m = 50, C_d = 10, k = 1)$, and c) $(K_m = 50, K_s = 20, k = 1)$

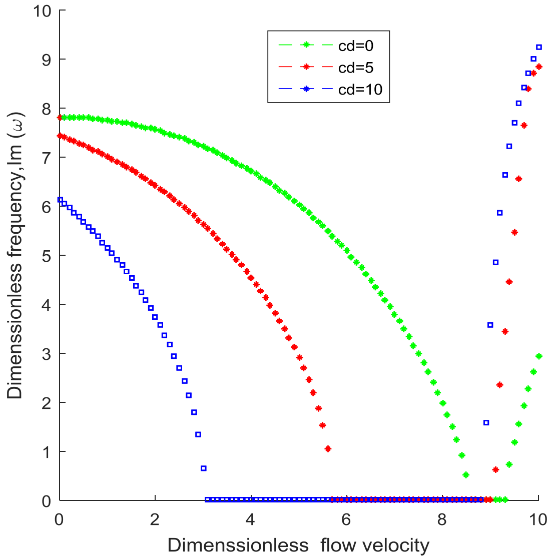

Fig. 7: Effect of damping foundation parameter on first natural frequency for (C-F) FG pipe with different flow velocity.

(**Fig. 7**) illustrate the effect of damping coefficient C_d on the dimensionless frequency and damping parts of fundamental eigenvalues of cantilever FG pipe conveying flow. Here, the results are presented for different dimensionless damping parameters, $C_d = 0$, $C_d = 5$ and $C_d = 10$. In this case, $K_m = 50$, $K_s = 20$ and gradient index $k = 1$. According to **Figs. 7**, the damping property of the viscoelastic foundation tends to decrease the bending stiffness of the FG pipe conveying flow. However, as can be seen, for a damped system, the bifurcation point happened earlier than system without damping, while the buckling instability and resonance frequency occur for multi values of damping coefficients and both the imaginary and the real parts of eigenvalue reach zero at this point. It is remarkable to note that increment the damping coefficient causes to induce the damping force and consequently the absorption of vibration energy by the structure is increased. It is worth mentioning that with increasing damping foundation, system stability decreased and becomes susceptible to buckling.

4- Conclusions

The dynamic behavior of cantilevered FG pipe conveying flow on the visco-elastic foundation is investigated in this paper. The properties of the material change constantly across the pipes thickness and depend on power law distribution. The vibration equations based on the Euler-Bernoulli beam theory and solved numerically using the DQ method. The numerical results show:

1- The DQM is more successful to solve the dynamic problem of FG pipe conveying fluid as compared to others method.

2- As the gradient index increases, the vibration frequency of the FGM flow pipe and the critical velocity of the (C-F) boundary will increase. In this way, we can improve the vibration and stability characteristics of the flow pipe by adjusting the gradient distribution of the FGM pipe material.

3- Increasing K_m and K_s leads to improved stiffness of system and consequently the stability increases while the imaginary part of frequency decreases with an increase of foundation viscous damping C_d.

NOMENCLATURE

Symbol	Description	Units

A_p , A_f	Cross-sectional area of the FG pipe and the fluid	m^2
C_d	damping coefficient of foundation	Pa. s
$C_{ij}^{(m)}$	Coefficient of differential quadrature	-----
$E(n)$	Modulus of elasticity for materials	GPa
E_R	Ratio of ceramic to metal of modulus of elasticity	-----
$f_x^{(1)}(\eta)$	function of differential quadrature	-----
F^{ext}	Viscoelastic foundation force	N
I	Second moment of area	m^4
h	Thickness of pipe	m
h_R	Ratio of thickness to mean radius of pipe	----
k	Gradient index of FGM	------
K_m	Winkler stiffness	MPa
K_s	Foundation constant	KN
(k_s, k_m, C)	Dimensionless viscoelastic foundation	-----
L	Length of pipe	m
m_f	The mass density for fluid	Kg/m^3
m_p	Effective mass of pipe	Kg/m^3
$(n - s)$	Normal coordinate system	------
R_i , R_o	Inner and the outer radii	m
T_f	Kinetic energy for fluid of FGM pipe	$N.m^2/s^2$
T_p	Kinetic energy for pipe of FGM pipe	$N.m^2/s^2$
t	Time	sec
δT	Virtual work of kinetic energy	$N.m^2/s^2$
U_s	strain energy of FGM	$N.m^2/s^2$
u	Dimensionless of flow velocity	-----
$u_{(x,t)}$	Transverse displacements	m
δU_s	Virtual work of internal forces	N.m
(u, v, w)	Displacements along the coordinate directions (x, y, z)	------
V_f	Flow velocity of fluid	m/s
δW^{ext}	Virtual work viscoelastic foundation	N.m
(x, y, z)	Cartesian coordinate system	m
$(Y(s), Z(n))$	Coordinate point on normal coordinate system.	m
Greek Symbols		
$\rho(n)$	Density for materials	kg/m^3
ρ_R	Ratio of ceramic to metal density	-----
ε_x	Strain of FGM	----
σ_x	Stress of FGM	GPa
v	Poisson's ratio	-----
τ	Non dimensional time	------
$\alpha(n)$	Flexural stiffness	$GPa. m^2$
β	Mass ratio	-----
λ	Natural frequency	Rad/s

Reference

[1] Eslami, G., Maleki, V. A., & Rezaee, M. (2016). Effect of open crack on vibration behavior of a fluid-conveying pipe embedded in a visco-elastic medium. Latin American Journal of Solids and Structures, 13(1), 136-154.

[2] Chellapilla, K. R., & Simha, H. S. (2008). Vibrations of fluid-conveying pipes resting on two-parameter foundation. Open Acoustics Journal, 1, 24-33.

[3] Tornabene, F., Marzani, A., Viola, E., & Elishakoff, I. (2010). Critical flow speeds of pipes conveying fluid using the generalized differential quadrature method. Advances in Theoretical and Applied Mechanics, 3(3), 121-138.

[4] Lu, P., & Sheng, H. (2012). Exact eigen-relations of clamped-clamped and simply supported pipes conveying fluids. International Journal of Applied Mechanics, 4(03), 1250035.

[5] Al-Hilli, A. H. (2013). Free vibration characteristics of elastically supported pipe conveying fluid. ALNAHRAIN JOURNAL FOR ENGINEERING SCIENCES, 16(1), 9-19.

[6] Mostafa, N. H. (2014). Effect of a Viscoelastic foundation on the Dynamic Stability of a Fluid Conveying Pipe. International Journal of Applied Science and Engineering, 12(1), 59-74.

[7] Kesimli, A., Bağdatlı, S. M., Çanakcı, S., Kesimli, A., Bağdatlı, S. M., & Çanakcı, S. (2016). Free vibrations of fluid conveying pipe with intermediate support. Res. Eng. Struct. Mater, 2, 75-87.

[8] Zare, A., Eghtesad, M., & Daneshmand, F. (2017). Numerical investigation and dynamic behavior of pipes conveying fluid based on isogeometric analysis. Ocean Engineering, 140, 388-400.

[9] Yun-dong, L., & Yi-ren, Y. (2017). Vibration analysis of conveying fluid pipe via He's variational iteration method. Applied Mathematical Modelling, 43, 409-420.

[10] Hu, K., Dai, H. L., Wang, L., & Qian, Q. (2017). Dynamics and Stability of Pinned-Free Micro pipes Conveying Fluid. Journal of Mechanics, 1-7.

[11] Shahba, A., & Rajasekaran, S. (2012). Free vibration and stability of tapered Euler–Bernoulli beams made of axially functionally graded materials. *Applied Mathematical Modelling*, *36*(7), 3094-3111.

[12] Wattanasakulpong, N., Prusty, B. G., Kelly, D. W., & Hoffman, M. (2012). Free vibration analysis of layered functionally graded beams with experimental validation. *Materials & Design (1980-2015)*, *36*, 182-190.

[13] Piovan, M. T., & Sampaio, R. (2008). Vibrations of axially moving flexible beams made of functionally graded materials. Thin-Walled Structures, 46(2), 112-121.

[14] Sina, S. A., Navazi, H. M., & Haddadpour, H. (2009). An analytical method for free vibration analysis of functionally graded beams. Materials & Design, 30(3), 741-747.

[15] Alshorbagy, A. E., Eltaher, M. A., & Mahmoud, F. F. (2011). Free vibration characteristics of a functionally graded beam by finite element method. Applied Mathematical Modelling, 35(1), 412-425.

[16] Kim, Y. W. (2005). Temperature dependent vibration analysis of functionally graded rectangular plates. *Journal of Sound and Vibration*, *284*(3-5), 531-549.

[17] Vosoughi, A. R. (2016). Nonlinear free vibration of functionally graded Nano beams on nonlinear elastic foundation. Iranian Journal of Science and Technology, Transactions of Civil Engineering, 40(1), 23-32.

[18] Ebrahimi, F., & Barati, M. R. (2018). Effect of three-parameter viscoelastic medium on vibration behavior of temperature-dependent non-homogeneous viscoelastic nanobeams in a hygro-thermal environment. Mechanics of Advanced Materials and Structures, 25(5), 361-374.

[19] Wang, Z. M., & Liu, Y. Z. (2016). Transverse vibration of pipe conveying fluid made of functionally graded materials using a symplectic method. Nuclear Engineering and Design, 298, 149-159.

[20] Deng, J., Liu, Y., Zhang, Z., & Liu, W. (2017). Dynamic behaviors of multi-span viscoelastic functionally graded material pipe conveying fluid. Proceedings of the Institution of Mechanical Engineers, Part C: Journal of Mechanical Engineering Science, 231(17), 3181-3192.

[21] Tang, Y., & Yang, T. (2018). Post-buckling behavior and nonlinear vibration analysis of a fluid-conveying pipe composed of functionally graded material. Composite Structures, 185, 393-400.

[22] Tanigawa, Y., Akai, T., Kawamura, R., & Oka, N. (1996). Transient heat conduction and thermal stress problems of a nonhomogeneous plate with temperature-dependent material properties. *Journal of Thermal Stresses*, *19*(1), 77-102.

[23] Paidoussis, M. P. (1998). *Fluid-structure interactions: slender structures and axial flow* (Vol. 1). Academic press.

[24] Benjamin, T. B. (1962). Dynamics of a system of articulated pipes conveying fluid-I. Theory. *Proc. R. Soc. Lond. A*, *261*(1307), 457-486.

[25] Shu, C., & Du, H. (1997). A generalized approach for implementing general boundary conditions in the GDQ free vibration analysis of plates. *International Journal of Solids and Structures*, *34*(7), 837-846.

[26] Shu, C. (2000). *Differential quadrature and its application in engineering*. Springer Science & Business Media.

[27] Bellman, R., Kashef, B. G., & Casti, J. (1972). Differential quadrature: a technique for the rapid solution of nonlinear partial differential equations. *Journal of computational physics*, *10*(1), 40-52.

[28] Shu, C., & Du, H. (1997). Implementation of clamped and simply supported boundary conditions in the GDQ free vibration analysis of beams and plates. *International Journal of Solids and Structures*, *34*(7), 819-835.

[29] Kim, S., & Kim, S. D. (2009). Preconditioning on high-order element methods using Chebyshev–Gauss–Lobatto nodes. *Applied Numerical Mathematics*, *59*(2), 316-333.